The Detection of Micromolar Pericellular ATP Pool on Lymphocyte Surface by Using Lymphoid Ecto-Adenylate Kinase as Intrinsic ATP Sensor ▣

Gennady G. Yegutkin,* Andrey Mikhailov,† Sergei S. Samburski,* and Sirpa Jalkanen*

*MediCity Laboratory and Department of Medical Microbiology, Turku University and National Public Health Institute, FIN-20520 Turku, Finland; and †Turku Centre for Biotechnology, University of Turku/Åbo Akademi University, FIN-20521 Turku, Finland

Current models of extracellular ATP turnover include transient release of nanomolar ATP concentrations, triggering of signaling events, and subsequent ectoenzymatic inactivation. Given the high substrate specificity for adenylate kinase for reversible reaction (ATP + AMP ↔ 2ADP), we exploited lymphoid ecto-adenylate kinase as an intrinsic probe for accurate sensing pericellular ATP. Incubation of leukemic T- and B-lymphocytes with [^{3}H]AMP or [α-^{32}P]AMP induces partial nucleotide conversion into high-energy phosphoryls. This "intrinsic" AMP phosphorylation occurs in time- and concentration-dependent fashions via nonlytic supply of endogenous γ-phosphate–donating ATP, remains relatively resistant to bulk extracellular ATP scavenging by apyrase, and is diminished after lymphocyte pretreatment with membrane-modifying agents. This enzyme-coupled approach, together with confocal imaging of quinacrine-labeled ATP stores, suggests that, along with predominant ATP accumulation within cytoplasmic granules, micromolar ATP concentrations are constitutively retained on lymphoid surface without convection into bulk milieu. High basal levels of inositol phosphates in the cells transfected with ATP-selective human P2Y$_2$-receptor further demonstrate that lymphocyte-surrounding ATP is sufficient for triggering purinergic responses both in autocrine and paracrine fashions. The ability of nonstimulated lymphocytes to maintain micromolar ATP halo might represent a novel route initiating signaling cascades within immunological synapses and facilitating leukocyte trafficking between the blood and tissues.

INTRODUCTION

Extracellular ATP turnover involves a multistep cascade consisting of 1) nucleotide release and triggering of diverse signaling events via ligand-gated P2X or G protein–coupled P2Y purinergic receptors (Lazarowski *et al.,* 2003); 2) nucleotide inactivation and/or interconversion by nucleotide-converting ectoenzymes (Zimmermann, 2000; Yegutkin *et al.,* 2002); 3) interaction of the resulting adenosine with own G protein–coupled receptors (Ralevic and Burnstock, 1998); and finally, 4) adenosine uptake by the cell via equilibrative or Na$^+$-dependent nucleoside transporters (Griffith and Jarvis, 1996).

The appearance of ATP in the external milieu represents a critical component of signaling cascade. The resting cells can release ATP at basal "constitutive" rates (Lazarowski *et al.,*

2000), and this process is transiently intensified under various mechanical (shear stress, hypotonic swelling, stretching, hydrostatic pressure) and chemical (e.g., Ca^{2+}-mobilizing agonists) stimuli (Joseph *et al.,* 2003; Lazarowski *et al.,* 2003). Current studies on ATP release involve either agitation of cell suspensions/monolayers, followed by removal of bathing medium and bioluminescent detection of ATP content, or direct addition of luciferase/luciferin reagent to the cells for sensing ATP in real time (Schwiebert and Zsembery, 2003). However, several innovative techniques provide evidence that the released ATP is spatially confined within unstirred membrane layers, and therefore, bioluminescent measurements of bulk nanomolar ATP concentrations are unlikely to reflect actual nucleotide levels.

Particularly, by using atomic force microscopy in combination with myosin ATPase-coated sensor tip, accumulation of ATP has been shown on surface of CFTR-transfected airway epithelial cells (Schneider *et al.,* 1999). On stimulation of a single pancreatic β-cell with glucose or glibenclamide, local ATP concentrations of over 25 μM were recorded using the patch-clamp technique with "biosensor" PC12 cell expressing P2X$_2$ receptors (Hazama *et al.,* 1998). Although these approaches discerned micromolar ATP in the microenvironment surrounding living cells, sophisticated detection apparatus and the necessity for three-dimensionally fine-controlled micromanipulators to bring the sensor into close proximity of the target cell limits their application for routine measurements. Moreover, correct interpretation of biosensor cell-based data is hampered by potential desensi-

tization or self-activation of P2X receptors during simultaneous ATP release from sensor cell (Hayashi *et al.,* 2004).

Another approach includes selective targeting of luciferase to the cell surface. The experiments of Dubyak and coworkers with membrane-attached protein A-luciferase revealed transient local release of 15–20 μM ATP from thrombin-activated platelets (Beigi *et al.,* 1999) and further demonstrated ATP segregation in the vicinity of human astrocytoma cells upon challenging with Ca^{2+}-mobilizing agonists (Joseph *et al.,* 2003). By using recombinant membrane-targeted luciferase, local release of 100–200 μM ATP was also detected in HEK293 cells in response to P2X$_7$ activation (Pellegatti *et al.,* 2005). A limitation of these assays is the need for specially designed surface antigens or cell lines appropriate for luciferase targeting. Moreover, by measuring the relative increases in light output or second messenger production, these techniques estimated only transient local ATP release from the stimulated cells.

Our recent TLC assays revealed that adenylate kinase (AK)-positive lymphocytes slightly converted [^{3}H]AMP into [^{3}H]ADP/ATP even without exogenous γ-phosphate–donating ATP (Yegutkin *et al.,* 2002; Henttinen *et al.,* 2003). Given the high substrate specificity for AK for the reversible reaction ATP + AMP $\leftrightarrow$ 2ADP (Yan and Tsai, 1999), we hypothesized that lymphoid ecto-AK may serve as an intrinsic probe for sensing cell-surrounding ATP. Here we showed that nonstimulated lymphocytes continuously retain pericellular ATP at concentrations sufficient for triggering purinergic responses. These findings provide a novel insight into the mechanism of cellular ATP turnover.

MATERIALS AND METHODS

Reagents

[2-^{3}H]AMP (spec. act. 19.7 Ci/mmol) and [α-^{32}P]AMP (0.5–3 Ci/mmol) were from Amersham Biosciences (Little Chalfont, Buckinghamshire, United Kingdom). [γ-^{32}P]ATP (3000 Ci/mmol) and *myo*-[2-^{3}H]inositol (18.5 Ci/mmol) were from Perkin Elmer Life Sciences (Boston, MA). Annexin V-FITC was from Alexis (Läufelfingen, Switzerland). Alexa Fluor555 conjugate of cholera toxin subunit-B (CTB) from *Vibrio cholera*, 7-aminoactinomycin-D (7-AAD) and acridine orange were from Molecular Probes Europe BV (Leiden, The Netherlands). ATP kit was from BioThema AB (Haninge, Sweden). TLC plates were Alugram SIL G/UV$_{254}$ and Polygram CEL-300 PEI types supplied by Macherey-Nagel (Duren, Germany). Free fatty acids were purchased from Sigma and stored at −70°C in stock 25 mM ethanol solutions. Soluble apyrase from potato (grade III), Dowex 1X8–200 ion-exchange resin, quinacrine, methyl-β-cyclodextrin, and all nucleotides were from Sigma (St. Louis, MO).

Cell Culture and Transfections

Human leukemic T-cell lymphoblast line Jurkat, derivative Jurkat mutant J.CaM1.6 deficient in *lck* kinase (JCaM), B-cell lymphoma line Namalwa and Chinese hamster ovary (CHO) cells were from ATCC (Manassas, VA). The Jurkat-CD73 transfectants (B-NT5.1) stably expressing glycosyl-phosphatidylinositol (GPI)-anchored 5'-nucleotidase/CD73 (Resta *et al.,* 1994) were kindly provided by Dr. Linda Thompson (Oklahoma Medical Research Foundation, Oklahoma City, OK). Lymphocytes were grown in RPMI-1640 with 10% fetal calf serum (FCS), 4 mM L-glutamine, 100 U/ml penicillin, 100 μg/ml streptomycin, and 400 μg/ml G-418 (in case of B-NT5.1 cells). The cells were also transfected with plasmid of human P2Y$_2$ receptor (Parr *et al.,* 1994), cloned in the pEGFP-N1 vector (gift of Dr. Wanda O'Neal, University of North Carolina, Chapel Hill, NC). Lymphocytes (5 × 10^6 cells) were transfected with 15 μg pEGFP-N1/P2Y$_2$-R cDNA by electroporation (850 V/cm, 1 mFa) and, after 48 h, selected for 1–2 wk with 0.4 mg/ml G-418. CHO cells growing in six-well plates were transfected with 6 μg pEGFP-N1/P2Y$_2$-R with Lipofectamine 2000 (Invitrogen, Carlsbad, CA) following the manufacturer's instructions. Geneticin-resistant CHO-P2Y$_2$-R cells were selected for 3–4 wk with medium containing 1 mg/ml G-418. Peripheral blood lymphocytes (PBL) were isolated from the venous blood of healthy human volunteers using Ficoll centrifugations.

Transphosphorylation of ^{32}P-labeled and Unlabeled Nucleotides

Jurkat and Namalwa (1 × 10^5 cells) were incubated for 12 min at 37°C in 80 μl RPMI-1640 containing 1 mM β-glycerophosphate, 10 μM ATP with tracer

[γ-^{32}P]ATP, and 200 μM AMP/NDP. Aliquots of the mixture were spotted onto Polygram TLC sheets and separated with 0.75 M KH$_2$PO$_4$ (pH 3.5) as solvent. Lymphocytes were also incubated for 50 min at 37°C in 80 μl RPMI-1640 containing 1 mM β-glycerophosphate, 0–100 μM ATP, and 10–100 μM AMP with tracer [α-^{32}P]AMP. Aliquots were spotted onto Alugram sheets, separated by TLC (Norman *et al.,* 1974), and developed by autoradiography.

Measurement of Ectoenzymatic [^{3}H]AMP Phosphorylation

The lymphocytes (2 × 10^5 cells) were incubated at 37°C in a final volume of 80 μl RPMI-1640 with 5 mM β-glycerophosphate in the following two ways: 1) for evaluation of intrinsic AMP phosphorylation, cells were incubated with 1–200 μM [^{3}H]AMP and 2) for measurement of specific AK activity, the assay buffer contained 400 μM [^{3}H]AMP plus 800 μM ATP. After a 45-min incubation, [^{3}H]AMP and its [^{3}H]metabolites were separated by TLC (Norman *et al.,* 1974) and quantified by scintillation β-counting (Yegutkin *et al.,* 2002).

Bioluminescent Quantification of Extracellular ATP

Lymphocytes (5 × 10^5 cells) were resuspended in 200 μl RPMI-1640 and incubated in 24-well plates for 45 min at 37°C. Aliquots of the bathing medium (40 μl) were clarified by centrifugation, and extracellular ATP was assayed by luciferin-luciferase luminometry using a TECAN-Ultra fluoropolarimeter (Yegutkin *et al.,* 2001).

Flow-Cytometric Analysis

For viability tests, lymphocytes (5 × 10^5 cells) were incubated for 90 min at 37°C in 0.5 ml RPMI-1640 medium containing 100 μM AMP. The cells were then washed, resuspended in 400 μl phosphate-buffered saline (PBS) containing 2% FCS, 0.01% NaN$_3$, 1 μl annexin V-FITC and 10 μg/ml 7-AAD, and analyzed using FACSCalibur with CellQuest-Prosoftware (Becton Dickinson, Mountain View, CA). The percentage of pEGFP-N1/P2Y$_2$-positive cell transfectants was also determined by flow cytometry.

Inositol Phosphate Assay

Wild-type and P2Y$_2$-transfected CHO cells were grown to confluence in 24-well tissue culture plates and radiolabeled by incubating in a humidified CO$_2$ incubator for 22 h with 250 μl inositol-free Dulbecco's modified Eagle's medium (DMEM) and 0.7 μCi *myo*-[^{3}H]-inositol. Exogenous nucleotide agonists and lymphoid cell suspensions were then added to the plates in 50 μl DMEM and incubated at 37°C for 5 and 30 min, respectively. The medium was aspirated, and the assay was terminated by adding 0.5 ml ice-cold 50 mM formic acid. After 20-min incubation on ice, cell extract was neutralized by 0.125 ml 150 mM NH$_4$OH and [^{3}H]inositol phosphates were resolved using Dowex 1X8-columns, as described previously (Lazarowski *et al.,* 1995). Likewise, Jurkat and Namalwa cells and their P2Y$_2$-transfectants were radiolabeled by incubating 1.5–2 × 10^5 lymphocytes in DMEM with 1 μCi *myo*-[^{3}H]-inositol. To avoid undesirable release of intracellular ATP from the mechanically disturbed lymphocytes, formic acid was added directly to the labeling medium without washing the cells.

Confocal Microscopy

The lymphocytes (5 × 10^5 cells) were incubated for 10–15 min at RT in 0.5 ml PBS containing 0.2% BSA and certain fluorochrome, washed twice, resuspended in 200 μl PBS/BSA, and placed into glass-bottom microwell dishes (MatTek, Ashland, MA). A confocal spectral laser-scanning microscope (LSM-510; Zeiss, Oberkochen, Germany) equipped with Argon and HeNe lasers and 63× 1.4 oil DIC objective was used to monitor fluorescent signals. Alexa$_{555}$-CTB (0.5 μg/ml) was used to label cell surface glycosphingolipids, and upon excitation with 543 nm, fluorescence was detected at >560 nm. For detection of putative ATP stores, the cells were incubated with 4 μM quinacrine, and fluorescence was detected at 500–530 nm with 477-nm excitation wavelengths. Acidic organelles were detected by using 4 μM acridine orange and fluorescence was detected at 500–530 and 650–710 nm with 477- and 488-nm excitations, respectively. The labeled lymphocytes were also pretreated for 30 min at RT with 10 mM methyl-β-cyclodextrin before microscopic inspection.

Data Analyses

The maximum [^{3}H]AMP-phosphorylating capacities (B$_{max}$) were determined using nonlinear least-squares curve fitting. Objective statistical criteria (F-test, extra sum of squares principle) were used for discriminating between one- and two-site models (Prism 4.02; GraphPad, San Diego, CA). Statistical comparisons were made using Student's *t* test, and $p < 0.05$ was taken as significant.

RESULTS

Coexistence of ATP-consuming and -regenerating Pathways on the Lymphoid Cell Surface

We took advantage of radio-TLC for evaluating the nucleotide-converting ectoenzymatic pathways, and Figure 1A
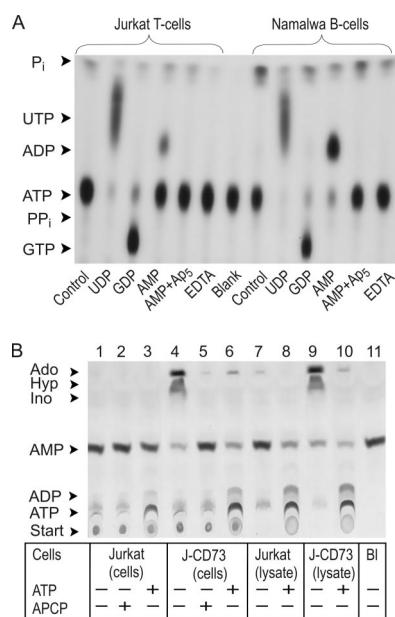
Figure 1. Metabolism and interconversion of exogenous nucleotides by lymphoid cells. (A) Jurkat and Namalwa cells were incubated for 12 min with 10 μM [γ-^{32}P]ATP and 200 μM UDP, GDP, and AMP, as indicated. The cells were also pretreated with 100 μM Ap_5A or 2.5 mM EDTA for 15 min at 37°C before addition of nucleotides. (B) Intact Jurkat cells, Jurkat CD73-transfectants (J-CD73), and their sonicated lysates were incubated for 45 min with 50 μM [^{3}H]AMP in the presence of 500 μM ATP and 30 μM APCP. Aliquots of the mixture were spotted onto PEI-cellulose (A) or SIL-G/UV$_{254}$ (B) plates, separated by TLC, and developed by autoradiography. Arrows indicate the positions of nucleotide standards, inorganic phosphorus (P_i), adenosine (Ado), inosine (Ino), and hypoxanthine (Hyp). The blanks (Bl) show the radiochemical purity of radiolabeled nucleotides after incubation without lymphoid cells.

illustrates the pattern of [γ-^{32}P]ATP metabolism by Jurkat and Namalwa cells. The lymphocytes directly converted [γ-^{32}P]ATP to ^{32}P$_i$ without any formation of ^{32}PP$_i$, thus indicating that ATP-hydrolyzing activity in lymphoid cells is represented by nucleoside triphosphate diphosphohydrolase (NTPDase) rather than by nucleotide pyrophosphatases/phosphodiesterases. EDTA markedly diminished this nucleotidase reaction, showing the Ca^{2+}-Mg^{2+} dependency of lymphoid NTPDases. Lymphocyte incubation with 10 μM [γ-^{32}P]ATP together with 200 μM UDP or GDP activated formation of the corresponding [γ-^{32}P]NTP via backward NDP kinase reaction. Joint addition of [γ-^{32}P]ATP and AMP stimulates their transphosphorylation into [β-^{32}P]ADP, which can be prevented by AK inhibitor Ap$_5$A.

Use of [^{3}H]AMP as another tracer substrate revealed that CD73-negative Jurkat were unable to hydrolyze [^{3}H]AMP (Figure 1B, lane 1), but instead, activated its interconversion with exogenous ATP via backward AK reaction (lane 3). Together, these autoradiographic data corroborate our previous competitive and substrate-specificity enzyme assays (Yegutkin *et al.*, 2002), showing that lymphoid cells are generally characterized by "ATP-regenerating phenotype" with high ecto-AK and NDP kinase activities and relatively low or even lacking expressions of NTPDases and ecto-5'-nucleotidase.

Lymphocytes Phosphorylate Tracer AMP Even without Exogenous γ-Phosphate–donating ATP

The autoradiography in Figure 1B additionally elicited slight but clearly detectable formation of ^{3}H-labeled

ADP/ATP after Jurkat incubation with [^{3}H]AMP (lane 1). A similar pattern of [^{3}H]AMP phosphorylation was observed earlier in the experiments with Namalwa B-cells, but not with cultured human umbilical vein endothelial cells (Yegutkin *et al.*, 2002; Henttinen *et al.*, 2003). Because these phosphotransfers occur without exogenous γ-phosphate–donating ATP, this phenomenon can be reasonably designated as an "intrinsic" AMP phosphorylation by lymphocytes.

To assess the potential impact of counteracting AMP-degrading pathway on the ability of lymphocytes to phosphorylate [^{3}H]AMP, we used Jurkat transfectants B-NT5.1 stably expressing ecto-5'-nucleotidase/CD73 (Resta *et al.*, 1994). Unlike parental CD73-negative Jurkat, B-NT5.1 efficiently converted radiolabeled AMP via adenosine into inosine/hypoxanthine (Figure 1B, lane 4). Pretreatment of B-NT5.1 cells with known competitive inhibitors of ecto-5'-nucleotidase, α,β-methylene-ADP (APCP) and ATP (Henttinen *et al.*, 2003), completely abrogated their AMP-hydrolyzing activity (lanes 5 and 6). Strikingly, along with prominent ATP-dependent [^{3}H]AMP phosphorylation via ecto-AK reaction (lane 6), these CD73-transfectants were still capable of slightly phosphorylating [^{3}H]AMP alone, irrespective of high ecto-5'-nucleotidase activity (lane 4).

Because nonspecific leakage of ATP may potentially contribute to the above [^{3}H]AMP phosphorylation, we used several independent approaches to assess this possibility. First, massive liberation of endogenous ATP was intentionally provoked by disruption of lymphocytes, accompanied by simultaneous releases of intracellular AK (Figure 1B, lanes 8 and 10) and other purinergic enzymes (Yegutkin *et al.*, 2002). However, the extents of intrinsic [^{3}H]AMP phosphorylation by sonicated Jurkat (Figure 1B, lane 7) and Jurkat-CD73 (lane 9) lysates were even diminished compared with intact lymphocytes (lanes 1 and 4). Second, we used a high-affinity phosphatidylserine-binding protein annexin-V that is rapidly translocated during apoptosis from the inner to the outer membrane leaflet. Flow-cytometric analysis of annexin-V staining, in combination with a marker of cell necrosis 7-AAD, confirmed that more than 95% of Jurkat remained viable after treatment with AMP (Figure 2A).

Use of AMP with ^{3}H-labeled adenine ring also does not exclude the theoretical possibility of moderate [^{3}H]AMP breakdown, following which the formed ^{3}H-labeled nucleosides are uptaken by lymphocytes, rephosphorylated into [^{3}H]ADP/ATP, and released into external milieu as a secondary event. Though, it seems highly unlikely for the following reasons. Both Jurkat and Namalwa lack ecto-5'-nucleotidase, whereas possible contribution of nonspecific phosphatases to the [^{3}H]AMP breakdown was excluded by supplementing the assay buffer with excess of alternative phosphorylated substrate, β-glycerophosphate. Most importantly, the employment of [α-^{32}P]AMP as another phosphate-accepting substrate unequivocally confirmed that lymphocytes directly phosphorylate tracer AMP into ADP in the absence of exogenous ATP, and this phosphotransfer occurs in a concentration-dependent manner, requires divalent cations, and is inhibited by Ap$_5$A (Figure 2B). Taken together, these data show that lymphocyte activate ecto-AK–mediated phosphorylation of tracer AMP via constitutive supply of endogenous γ-phosphate donating ATP, which occurs not as a consequence of cell lysis or plasma membrane damage.
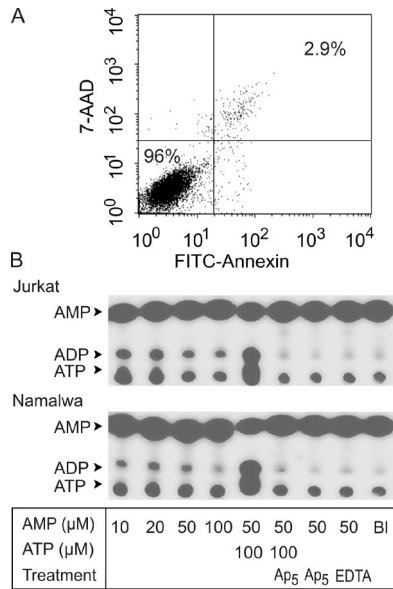
Figure 2. Pattern of $[\alpha\text{-}^{32}P]$AMP phosphorylation by lymphocytes. (A) Jurkat cells were incubated for 90 min with 100 μM AMP, and their viability was assessed by double staining with a marker of apoptosis annexin V-FITC (abscissa) and cell-impermeable dye 7-AAD (ordinate). The percentages of viable and necrotic cells are shown in the bottom left and top right quadrants of the dot plot graph, respectively. (B) Jurkat (top panel) and Namalwa (bottom panel) were incubated for 50 min with tracer $[\alpha\text{-}^{32}P]$AMP and the indicated concentrations of unlabeled AMP and ATP. Cells were also pretreated with 50 μM Ap$_5$A (Ap$_5$) or 2.5 mM EDTA before addition of nucleotide substrates. Mixture aliquots were spotted onto SIL-G/UV$_{254}$ plates, separated by TLC, and developed by autoradiography.

Evidence that Lymphocytes Maintain Micromolar Pericellular ATP without Significant Nucleotide Convection into Bulk Milieu

Further quantitative TLC analysis confirmed progressive $[^3H]$AMP conversion into $[^3H]$ADP/ATP by Jurkat cells, which reached a plateau value after a 45-min incubation (Figure 3A). Similar time courses for ATP-mediated $[^3H]$AMP phosphorylation has been shown earlier for endothelial (Yegutkin *et al.,* 2001) and lymphoid (Yegutkin *et al.,* 2002) ecto-AK. The prolonged dynamics of $[^3H]$AMP phosphorylation is presumably defined by the necessity for optimal binding and orientation of the phosphate acceptor relative to the phosphate being transferred via AK reaction (Yan and Tsai, 1999).
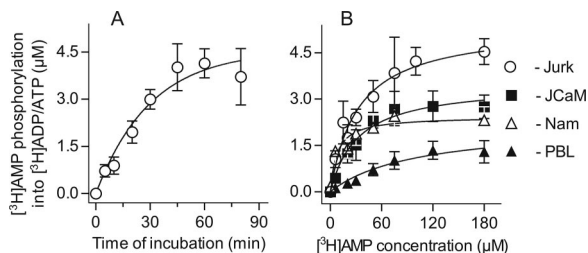

Figure 3. Kinetics of $[^3H]$AMP phosphorylation by lymphoid cells. (A) Time course of conversion of 50 μM $[^3H]$AMP into $[^3H]$ADP/ATP by Jurkat cells (mean $\pm$ SEM; n = 4). (B) The extent of $[^3H]$AMP phosphorylation versus substrate concentration plots. Values are the mean $\pm$ SEM for Jurkat (Jurk; n = 8), *lck*-deficient Jurkat mutants J.CaM1.6 (JCaM; n = 3), Namalwa (Nam; n = 3), and freshly isolated human PBL (n = 3).
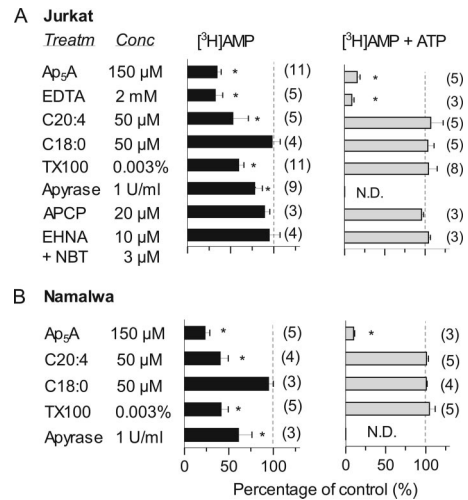
Figure 4. Effect of various agents on intrinsic $[^3H]$AMP-phosphorylating capacity and adenylate kinase activity in lymphocytes. Jurkat (A) and Namalwa (B) were pretreated for 20 min with the indicated compounds followed by addition of either 50 μM $[^3H]$AMP alone (■) or 400 μM $[^3H]$AMP plus 800 μM ATP (▥) for measuring the intrinsic AMP-phosphorylating capacity and specific ecto-AK activity, respectively. The amount of $[^3H]$AMP converted into $[^3H]$ADP/ATP after a 45-min incubation with lymphocytes was determined by TLC and is represented as percentage of controls (mean $\pm$ SEM), with the number of experiments in parentheses. * p < 0.05 compared with nontreated control cells. ND, not determined.

Steady-state analysis was then performed by incubating lymphocytes with $[^3H]$AMP and the increasing concentrations of unlabeled AMP for 45 min, until saturation was achieved (Figure 3B). Fitting the constructed concentration-response curves to a one-site model determined the following maximum $[^3H]$AMP-phosphorylating capacities for Jurkat, Namalwa, *lck*-deficient Jurkat mutants JcaM, and human PBL: 5.37 $\pm$ 0.58, 2.36 $\pm$ 0.25, 3.47 $\pm$ 0.43, and 1.8 $\pm$ 0.58 μM. In the presence of high saturated concentrations of $[^3H]$AMP, the extent of its transphosphorylation is mainly restricted by the limited source of endogenous ATP available as an alternative source of γ-terminal phosphate. With this assumption, the computed B_{max} values can be reasonably interpreted as total amount of cell-derived ATP transphosphorylated with tracer AMP through lymphoid ecto-AK reaction. Notably, these values significantly exceed bulk extracellular ATP measured by using conventional bioluminescent assay and equal to 42 $\pm$ 16 and 36 $\pm$ 10 nM (n = 5) for Jurkat and Namalwa, respectively. These kinetic data suggest that lymphoid cells constitutively maintain pericellular ATP at certain characteristic micromolar levels, without significant nucleotide convection into bulk milieu.

Membrane-modifying Agents Diminish the Intrinsic $[^3H]$AMP-phosphorylating Capacity of Lymphocytes without Affecting Ecto-adenylate Kinase Activity

We then evaluated the effects of various agents on the extent of $[^3H]$AMP phosphorylation by lymphocytes. To exclude the undesirable leakage of intracellular nucleotide kinases and/or spurious effects of certain reagents on AMP-phosphorylating capability of the treated cells, lymphoid AK was concurrently assayed by using saturating concentrations of $[^3H]$AMP plus ATP. In support of autoradiographic data with $[\alpha\text{-}^{32}P]$AMP shown in Figure 2B, cation-chelating agent EDTA and bisubstrate analogue Ap$_5$A inhibited both intrin-
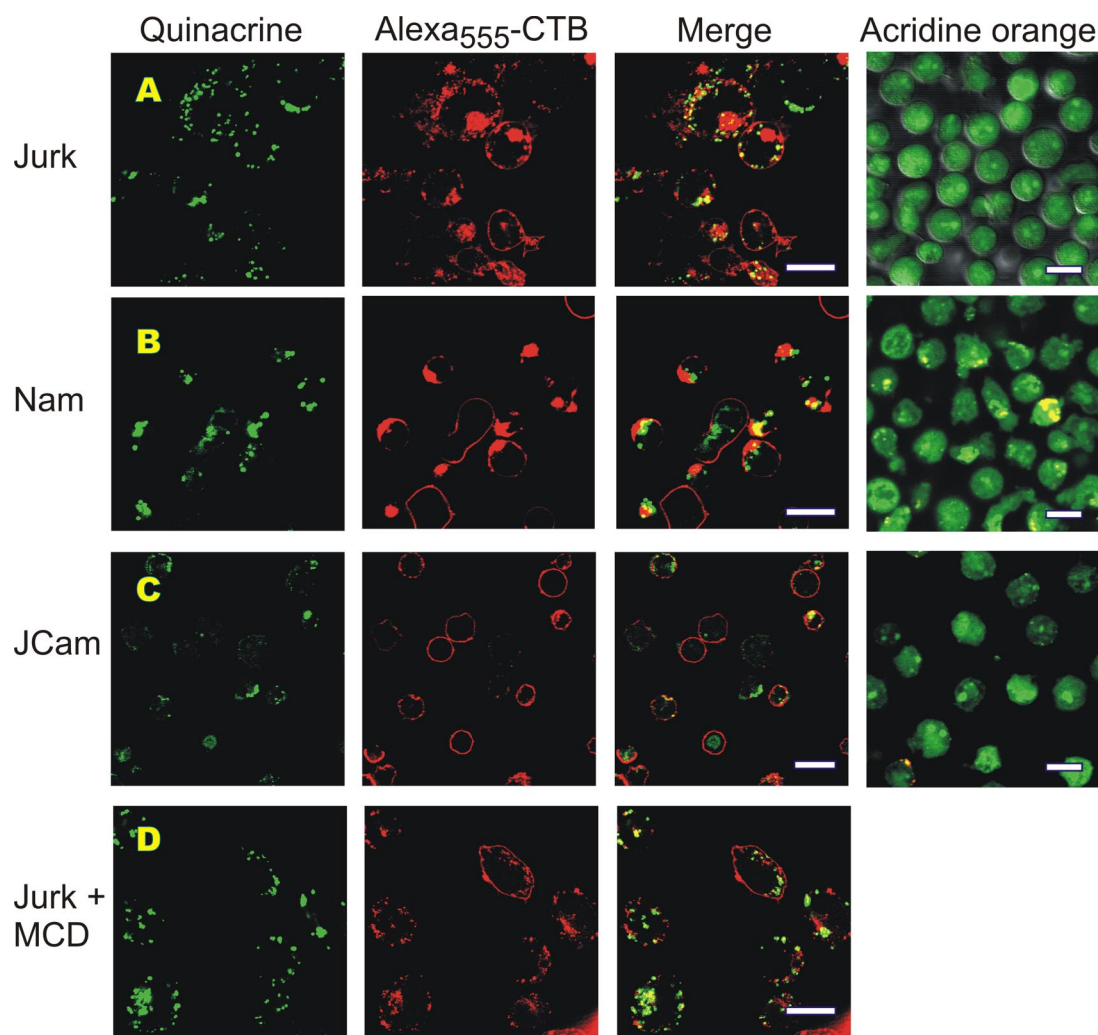
Figure 5. Confocal microscopic analysis of putative ATP stores in lymphocytes. Live Jurkat T-cells (A), Namalwa B-cells (B), and *lck*-deficient Jurkat mutants J.CaM (C) were costained with cell surface marker Alexa$_{555}$-CTB (red) and marker of putative ATP stores quinacrine (green), as well as with another acidotropic dye acridine orange. (D) CTB- and quinacrine-labeled Jurkat were pretreated for 30 min with 10 mM methyl-β-cyclodextrin (MCD) before microscopic inspection. Z-stack reconstruction of the adjacent images of Jurkat cells costained with Alexa$_{555}$-CTB and quinacrine can also be viewed in movie format in the Supplementary Video. Bar, 10 μm.

sic and ATP-stimulated [3H]AMP phosphorylation (Figure 4), thus confirming that these reactions occur via the same AK-mediated mechanism.

Treatment of lymphocytes with polyunsaturated arachidonic fatty acid (C20:4) and another membrane-modifying agent Triton X-100, but not with saturated stearic fatty acid (C18:0), significantly diminished their intrinsic [3H]AMP-phosphorylating capacity without affecting AK activity per se (Figure 4). Notably, Triton X-100 was used at low sub-solubilizing concentration (0.003% or ~50 μM), which is much lower than critical constant of micelle formation equal for this nonionic detergent to 0.015% (Helenius and Simons, 1975). Surprisingly, soluble apyrase only partially prevented [3H]AMP phosphorylation, thus suggesting the existence of apyrase-resistant ATP pool in the lymphocyte environment (concurrent measurement of AK was compromised by rapid scavenging of exogenous ATP by apyrase). The extent of [3H]AMP phosphorylation remained unchanged after Jurkat treatment with the inhibitors of nucleoside transport (NBT) and adenosine deaminase (EHNA; Figure 4A). Importantly, use of competitive ecto-5'-nucleotidase inhibitor APCP at

concentrations sufficient to block [3H]AMP hydrolysis does not affect [3H]AMP-phosphorylating capacities of both wild-type Jurkat and CD73-transfected B-NT5.1 cells (Figures 1B and 4A). Hence, in the presence of APCP, this technique may also be applied for detecting ATP in the vicinity of various CD73-positive cells.

Lymphocytes Store Cellular ATP in Cytoplasmic Granules beneath Plasma Membrane Patches

For visualization of cellular ATP, we used fluorescent dye quinacrine that belongs to the quinoline-acridine class, binds to nucleic acids, and is considered as the preferred available marker for detecting releasable ATP stores (Mitchell *et al.,* 1998; Sorensen and Novak, 2001). The quinacrine-labeled cells were also costained with CTB, which binds to the pentasaccharide chain of ganglioside G_{M1} and is widely used as a marker of glycosphingolipid-rich domains in lymphocytes (Harder *et al.,* 1998; Janes *et al.,* 1999). Costaining of Jurkat with quinacrine and Alexa$_{555}$-CTB revealed the accumulation of green quinacrine fluorescence within granular vesicles, which significantly coincide with red CTB-labeled

Figure 6. Characterization of inositol phosphate formation in the cells expressing human P2Y$_2$ receptor. CHO (A), Namalwa (B), and Jurkat (C) cells were transfected with pEGFP-N1/hP2Y$_2$-R cDNA, and the fluorescence histograms for wild-type (gray filling) and hP2Y$_2$-R-transfected (bold line) cells are shown. (D) Wild-type CHO and CHO-P2Y$_2$-R cells, labeled overnight with [^{3}H]inositol, were incubated with exogenous nucleotide agonists and lymphocyte suspensions for 5 and 30 min, respectively. Nucleotide concentrations and lymphocyte amounts are indicated as μmol/L and 10^6 cells/well. (E) Namalwa (Nam) and Jurkat (Jur) cells and their P2Y$_2$-R transfectants were also radiolabeled with [^{3}H]inositol and incubated without and with 1–10 μM ATP. [^{3}H]inositol phosphates were quantified by ion-exchange chromatography. The data are mean $\pm$ SEM (n = 3–5). * p < 0.05 compared with nontreated controls. ** p < 0.05 for P2Y$_2$-R-transfectants compared with wild-type cells.
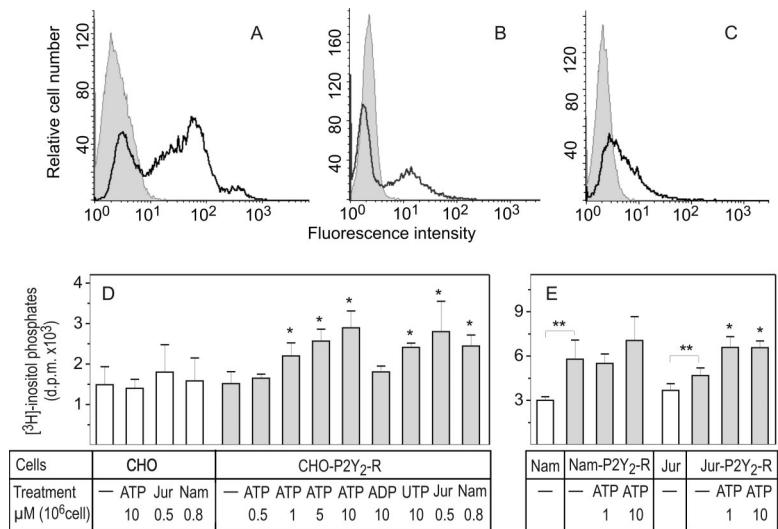
patches (Figure 5A). Computer reconstructions of these signals from serial confocal images along the *z*-axis further demonstrated that cytoplasmic quinacrine-stainable vesicles are mainly concentrated beneath CTB-labeled plasma membrane microdomains (Supplementary Video). Likewise, Namalwa also accumulated quinacrine within granular vesicles with significant colocalization of green quinacrine and red Alexa$_{555}$-CTB fluorescences (Figure 5B), whereas *lck*-deficient JCaM cells displayed fainter quinacrine staining and more homogenous surface distribution of Alexa$_{555}$-CTB (Figure 5C).

Notably, previous studies with relatively high concentrations of CTB (10–15 μg/ml) were able to visualize membrane microdomains on Jurkat surface only under conditions of aggregation of the T-cell antigen receptor or cross-linking of GPI-anchored proteins (Harder *et al.*, 1998; Janes *et al.*, 1999). Here we show that at very low concentrations (0.5 μg/ml), Alexa$_{555}$-CTB can also be concentrated to distinct patches on surface of nonstimulated lymphocytes. We also examined the patching behavior and pattern of quinacrine staining after disrupting the membrane rafts with the known cholesterol-extracting agent methyl-β-cyclodextrin (Harder *et al.,* 1998; Janes *et al.,* 1999). In comparison to control Jurkat (Figure 5A), the CTB-labeled clusters in cholesterol-depleted Jurkat were smaller and more diffusely distributed over the cell surface, whereas the granular quinacrine staining remained unchanged (Figure 5D). These findings further confirm that the visualized CTB-labeled domains can be reasonably attributed to ganglioside-G$_{M1}$-enriched lipid rafts.

Because quinacrine is a weak base, we used another acidotropic probe acridine orange for control labeling and tracing acidic organelles. This dual-fluorescence dye undergoes a pH-dependent shift from the green to red-orange emission and a similar shift is seen when acridine orange binds to DNA and RNA. Unlike granular quinacrine accumulation, lymphocyte staining with acridine orange revealed more even green fluorescence with a few red spots (Figure 5, A–C), thus excluding the possibility of nonspecific quinacrine partitioning into cellular acidic compartments in our assays.

Lymphocytes Maintain Pericellular ATP at Concentrations Sufficient for Activation of Purinergic Receptors

To evaluate the ATP-mediated purinergic responses, the cells were then transfected with human P2Y$_2$ receptor, cloned in the

pEGFP-N1 vector. Figure 6 confirms the moderately high expression of hP2Y$_2$-R on surfaces of CHO (A), Namalwa (B), and to less extent, Jurkat (C) cells. Consistent with the previously reported agonist profile for human ATP/UTP-selective P2Y$_2$ receptors (Parr *et al.,* 1994; Lazarowski *et al.,* 1995), treatment of CHO-P2Y$_2$-R transfectants with the increasing micromolar concentrations of ATP caused progressive accumulation of [^{3}H]inositol triphosphates, and similar activation was observed in the presence of 10 μM UTP, but not ADP (Figure 6D). Strikingly, the lymphoid cells were also able to increase [^{3}H]inositol phosphates production in P2Y$_2$-R–transfected CHO cells, presumably in an ATP-dependent manner. Furthermore, unlike CHO cells where expression of P2Y$_2$ receptor did not affect phospholipase-C activity (Figure 6D), the basal level of [^{3}H]inositol phosphates in Jurkat- and especially Namalwa-P2Y$_2$-R transfectants was significantly higher than in wild-type controls (Figure 6E). Together, these functional assays support the above radio-TLC enzyme data on constitutive external ATP supply in the lymphocyte environment and further demonstrate that lymphocyte-surrounding ATP concentrations are sufficient for triggering purinergic responses both in paracrine and autocrine fashions. Noteworthy, micromolar concentrations of exogenous ATP additionally increased inositol phosphate levels in Jurkat-P2Y$_2$–R cells, but not in Namalwa transfectants (Figure 6E). Therefore, taking into account the phenomenon of agonist-mediated desensitization of P2Y$_2$ and other purinergic receptors (Lazarowski *et al.,* 1995), we do not exclude that continuous "self-activation" of lymphocytes by endogenously released ATP might substantially diminish the magnitude of purinergic signaling.

DISCUSSION

Current models of extracellular ATP turnover are thought to include transient release of nanomolar ATP concentrations and subsequent triggering of diverse signaling events. The principal finding of this work is that, by developing a novel radio-TLC assay with surface-associated AK as an intrinsic ATP sensor, we have shown that nonexcitatory lymphoid cells constitutively retain micromolar concentrations of ATP in their pericellular space, without significant nucleotide convection into bulk milieu.

Along with marked ATP-dependent nucleotide phosphorylation through sequential ecto-AK and NDP kinase reactions, the lymphocytes were able to slightly phosphorylate

[3]H- or ^{32}P-labeled AMP without exogenous γ-phosphate–donating ATP (Figures 1 and 2). This process occurs in a time- and concentration-dependent fashions, is not accompanied by any signs of cell lysis, and is mediated via direct ectoenzymatic transphosphorylation of tracer AMP with micromolar concentrations of lymphocyte-derived ATP. Although these studies were mostly performed with CD73-negative Jurkat T-cells and Namalwa B-cells where ecto-AK represents the major AMP-converting pathway, Jurkat CD73-transfectants and human PBL also phosphorylated [^{3}H]AMP to some extent, irrespective of the coexpression of counteracting enzyme ecto-5′-nucleotidase/CD73. Another important ectoenzyme to be taken into consideration is E-NTPDase/CD39, otherwise known as ecto-ATPase, apyrase (Zimmermann, 2000). Surprisingly, lymphocyte pretreatment with soluble apyrase only partially diminished their [^{3}H]AMP-phosphorylating capacity (Figure 4). Probably, unlike the bulk extracellular ATP pool, surface-localized ATP is somehow protected from apyrase scavenging. Likewise, recent assays with surface-attached luciferase demonstrated that, in response to mechanical or chemical stimuli, the platelets (Beigi *et al.,* 1999) and astrocytoma cells (Joseph *et al.,* 2003) release ATP, which is accumulated on the cell surface and remains relatively resistant to endogenous and exogenous nucleotidases.

AK is generally considered as classical intracellular enzyme that is localized in the cytosol (AK1), mitochondrial intermembrane space (AK2), and mitochondrial matrix (AK3; Yan and Tsai, 1999). However, plasma membrane–associated isoform AK1β has also been described (Collavin *et al.,* 1999; Ruan *et al.,* 2002), and the existence of cell surface-associated AK activity is currently appreciated (Yegutkin *et al.,* 2001; Picher and Boucher, 2003). Intracellular AK, in conjunction with NDP kinase, creatine kinase and glycolytic enzymes, play a critical role in energy transfer and distribution between mitochondria, cytosol, and nucleus (Dzeja and Terzic, 2003). Data on functional association of AK with ATP-sensitive potassium channels (Carrasco *et al.,* 2001) and intrinsic AK activity of cystic fibrosis transmembrane conductance regulator that controls gating of this anion channel in vivo (Randak and Welsh, 2003) provide additional evidence for communicating phosphotransfer signals to the membrane environments. The revealed here ability of lymphocytes to retain and/or transphosphorylate significant amounts of ATP and other nucleotides in the pericellular space allows to expand the above concepts by hypothesizing the coexistence of spatially arranged intra- and extracellular phosphotransfer networks coordinating both energetic homeostasis and signal transduction pathways.

Cellular mechanisms that underlie nonlytic ATP release might include 1) exocytosis of ATP-containing vesicles; 2) facilitated diffusion by nucleotide transporters or nucleotide/nucleoside exchangers; or 3) electrodiffusional movement through ATP-permeable anion channels (Lazarowski *et al.,* 2003; Schwiebert and Zsembery, 2003). Labeling of live lymphocytes with a marker of putative ATP stores quinacrine suggests the likely storage of ATP within cytoplasmic granules (Figure 5). Granular quinacrine staining has also been shown in experiments with rabbit ciliary epithelial cells (Mitchell *et al.,* 1998), human vascular endothelial cells (Bodin and Burnstock, 2001), and rat pancreatic acini (Sorensen and Novak, 2001). Stimulation of ATP release by various stimuli (hypotonic stress, shear stress, cholinergic stimulation) markedly decreased fluorescence intensity in these studies, thus confirming that quinacrine labels the releasable ATP stores. The important novelty of this work is the demonstration that quinacrine-stainable granules primarily coincide beneath Alexa[555]-CTB–labeled lymphoid membrane patches (Figure 5 and Online Video), which are enriched with ganglioside G_{M1} and can be reasonably attributed to lipid rafts. Interestingly, other purinergic molecules are also associated with lipid rafts and caveolae, including ATP permeation sites (Joseph *et al.,* 2003), P2Y (Kaiser *et al.,* 2002) and $P2X_3$ receptors (Vacca *et al.,* 2004), E-NTPDase/CD39 (Koziak *et al.,* 2000; Joseph *et al.,* 2003), and GPI-linked ecto-5′-nucleotidase/CD73 (Resta *et al.,* 1994).

The idea that lipid rafts may function as foci of ATP turnover is generally consistent with the important role of these membrane-specialized assemblies in signaling and membrane trafficking in lymphocytes (Janes *et al.,* 1999; Alonso and Millan, 2001). Specifically, polyunsaturated fatty acids markedly impaired the early steps of Jurkat T-cell activation, presumably via biosynthetic incorporation into membrane microdomains and displacement of LAT and Src kinases (Stulnig *et al.,* 2001) and coincidentally diminished the ability of lymphocytes to phosphorylate [^{3}H]AMP in our assays (Figure 4). Concurrent disturbances of T-cell receptor activation and cellular ATP turnover provide a novel insight into membrane mechanisms underlying the beneficial effects of polyunsaturated fatty acids in a variety of autoimmune and inflammatory disorders (Stulnig, 2003). Moreover, we have shown that *lck*-deficient JCaM cells are characterized by lower [^{3}H]AMP-phosphorylating capacity and fainter quinacrine staining, compared with parental Jurkat. These observations, together with data on strongly reduced amounts of tyrosine-phosphorylated proteins in these mutants (Harder and Simons, 1999), also suggest the existence of functional/structural interplay between ATP turnover and signaling machinery.

In view of the emerging proinflammatory role of ATP in the immune system, this model raises important questions regarding the physiological relevance of pericellular ATP pool. By measuring the basal and agonist-stimulated [^{3}H]inositol phosphate accumulation in the CHO and lymphoid cells transfected with ATP-selective $hP2Y_2$ receptor, here we also showed that lymphocytes constitutively supply external ATP at concentrations sufficient for promoting second-messenger responses both in autocrine and paracrine fashions (Figure 6). Pericellular ATP may serve as signaling loop sufficient for self-regulation of lymphocyte function and/or desensitization of purinergic receptors that particularly might explain why activation of lymphoid $P2X_7$ and other P2X receptors occurs only at high micromolar ATP concentrations (Di Virgilio *et al.,* 2001). Moreover, the ability of lymphocytes to retain micromolar ATP halo, in conjunction with leukocyte-governed suppression of endothelial ecto-5′-nucleotidase/CD73 (Henttinen *et al.,* 2003), could also represent a novel form of cross-talk between adherent leukocytes and targeted endothelium, thereby facilitating leukocyte trafficking between the blood and tissues.

In conclusion, by developing a novel enzyme-coupled ATP-sensing approach, in combination with confocal microscopic imaging, we have shown that lymphocytes maintain an ATP halo at certain micromolar levels and further suggest the likely recruitment of cellular ATP via cargo-vesicle trafficking and/or exocytotic granule secretion onto specific membrane microdomains. Unlike previous techniques with membrane-targeted luciferase and external biosensors (see *Introduction*), this radio-TLC assay provides a simple and reliable tool to quantify total amount of ATP in the vicinity of intact nonstimulated cells, without additional steps of cell transfections or other undesirable manipulations. As for the nanomolar ATP concentrations, which can be detected luminometrically as a "purinergic tone" (Lazarowski *et al.,* 2000), they probably reflect a minor fraction of the actual mass of cell-surrounding ATP, which is exchanged with

bulk phase via dissociation-association mechanisms and can be additionally shed from the membrane layers under various stimuli. Together, these findings provide sufficient justification for reexamination of current concepts of extracellular ATP turnover.

REFERENCES

Alonso, M. A., and Millan, J. (2001). The role of lipid rafts in signalling and membrane trafficking in T lymphocytes. J. Cell Sci. *114*, 3957–3965.

Beigi, R., Kobatake, E., Aizawa, M., and Dubyak, G. R. (1999). Detection of local ATP release from activated platelets using cell surface-attached firefly luciferase. Am. J. Physiol. *276*, C267–C278.

Bodin, P., and Burnstock, G. (2001). Evidence that release of adenosine triphosphate from endothelial cells during increased shear stress is vesicular. J. Cardiovasc. Pharmacol. *38*, 900–908.

Carrasco, A. J., *et al.* (2001). Adenylate kinase phosphotransfer communicates cellular energetic signals to ATP-sensitive potassium channels. Proc. Natl. Acad. Sci. USA *98*, 7623–7628.

Collavin, L., Lazarevic, D., Utrera, R., Marzinotto, S., Monte, M., and Schneider, C. (1999). wt p53 dependent expression of a membrane-associated isoform of adenylate kinase. Oncogene *18*, 5879–5888.

Di Virgilio, F., Chiozzi, P., Ferrari, D., Falzoni, S., Sanz, J. M., Morelli, A., Torboli, M., Bolognesi, G., and Baricordi, O. R. (2001). Nucleotide receptors: an emerging family of regulatory molecules in blood cells. Blood *97*, 587–600.

Dzeja, P. P., and Terzic, A. (2003). Phosphotransfer networks and cellular energetics. J. Exp. Biol. *206*, 2039–2047.

Griffith, D. A., and Jarvis, S. M. (1996). Nucleoside and nucleobase transport systems of mammalian cells. Biochim. Biophys. Acta *1286*, 153–181.

Harder, T., Scheiffele, P., Verkade, P., and Simons, K. (1998). Lipid domain structure of the plasma membrane revealed by patching of membrane components. J. Cell Biol. *141*, 929–942.

Harder, T., and Simons, K. (1999). Clusters of glycolipid and glycosylphosphatidylinositol-anchored proteins in lymphoid cells: accumulation of actin regulated by local tyrosine phosphorylation. Eur. J. Immunol. *29*, 556–562.

Hayashi, S., Hazama, A., Dutta, A. K., Sabirov, R. Z., and Okada, Y. (2004). Detecting ATP release by a biosensor method. Sci. STKE *2004*, pl14.

Hazama, A., Hayashi, S., and Okada, Y. (1998). Cell surface measurements of ATP release from single pancreatic beta cells using a novel biosensor technique. Pfluegers Arch. *437*, 31–35.

Helenius, A., and Simons, K. (1975). Solubilization of membranes by detergents. Biochim. Biophys. Acta *415*, 29–79.

Henttinen, T., Jalkanen, S., and Yegutkin, G. G. (2003). Adherent leukocytes prevent adenosine formation and impair endothelial barrier function by ecto-5′-nucleotidase/CD73-dependent mechanism. J. Biol. Chem. *278*, 24888–24895.

Janes, P. W., Ley, S. C., and Magee, A. I. (1999). Aggregation of lipid rafts accompanies signaling via the T cell antigen receptor. J. Cell Biol. *147*, 447–461.

Joseph, S. M., Buchakjian, M. R., and Dubyak, G. R. (2003). Colocalization of ATP release sites and ecto-ATPase activity at the extracellular surface of human astrocytes. J. Biol. Chem. *278*, 23331–23342.

Kaiser, R. A., Oxhorn, B. C., Andrews, G., and Buxton, I. L. (2002). Functional compartmentation of endothelial P2Y receptor signaling. Circ. Res. *91*, 292–299.

Koziak, K., *et al.* (2000). Palmitoylation targets CD39/endothelial ATP diphosphohydrolase to caveolae. J. Biol. Chem. *275*, 2057–2062.

Lazarowski, E. R., Boucher, R. C., and Harden, T. K. (2000). Constitutive release of ATP and evidence for major contribution of ecto-nucleotide pyrophosphatase and nucleoside diphosphokinase to extracellular nucleotide concentrations. J. Biol. Chem. *275*, 31061–31068.

Lazarowski, E. R., Boucher, R. C., and Harden, T. K. (2003). Mechanisms of release of nucleotides and integration of their action as P2X- and P2Y-receptor activating molecules. Mol. Pharmacol. *64*, 785–795.

Lazarowski, E. R., Watt, W. C., Stutts, M. J., Boucher, R. C., and Harden, T. K. (1995). Pharmacological selectivity of the cloned human P2U-purinoceptor: potent activation by diadenosine tetraphosphate. Br. J. Pharmacol. *116*, 1619–1627.

Mitchell, C. H., Carre, D. A., McGlinn, A. M., Stone, R. A., and Civan, M. M. (1998). A release mechanism for stored ATP in ocular ciliary epithelial cells. Proc. Natl. Acad. Sci. USA *95*, 7174–7178.

Norman, G. A., Follett, M. J., and Hector, D. A. (1974). Quantitative thin-layer chromatography of ATP and the products of its degradation in meat tissue. J. Chromatogr. *90*, 105–111.

Parr, C. E., Sullivan, D. M., Paradiso, A. M., Lazarowski, E. R., Burch, L. H., Olsen, J. C., Erb, L., Weisman, G. A., Boucher, R. C., and Turner, J. T. (1994). Cloning and expression of a human P2U nucleotide receptor, a target for cystic fibrosis pharmacotherapy. Proc. Natl. Acad. Sci. USA *91*, 3275–3279.

Pellegatti, P., Falzoni, S., Pinton, P., Rizzuto, R., and Di Virgilio, F. (2005). A novel recombinant plasma membrane-targeted luciferase reveals a new pathway for ATP secretion. Mol. Biol. Cell *16*, 3659–3665.

Picher, M., and Boucher, R. C. (2003). Human airway ecto-adenylate kinase. A mechanism to propagate ATP signaling on airway surfaces. J. Biol. Chem. *278*, 11256–11264.

Ralevic, V., and Burnstock, G. (1998). Receptors for purines and pyrimidines. Pharmacol. Rev. *50*, 413–492.

Randak, C., and Welsh, M. J. (2003). An intrinsic adenylate kinase activity regulates gating of the ABC transporter CFTR. Cell *115*, 837–850.

Resta, R., Hooker, S. W., Laurent, A. B., Shuck, J. K., Misumi, Y., Ikehara, Y., Koretzky, G. A., and Thompson, L. F. (1994). Glycosyl phosphatidylinositol membrane anchor is not required for T cell activation through CD73. J. Immunol. *153*, 1046–1053.

Ruan, Q., Chen, Y., Gratton, E., Glaser, M., and Mantulin, W. W. (2002). Cellular characterization of adenylate kinase and its isoform: two-photon excitation fluorescence imaging and fluorescence correlation spectroscopy. Biophys. J. *83*, 3177–3187.

Schneider, S. W., Egan, M. E., Jena, B. P., Guggino, W. B., Oberleithner, H., and Geibel, J. P. (1999). Continuous detection of extracellular ATP on living cells by using atomic force microscopy. Proc. Natl. Acad. Sci. USA *96*, 12180–12185.

Schwiebert, E. M., and Zsembery, A. (2003). Extracellular ATP as a signaling molecule for epithelial cells. Biochim. Biophys. Acta *1615*, 7–32.

Sorensen, C. E., and Novak, I. (2001). Visualization of ATP release in pancreatic acini in response to cholinergic stimulus. Use of fluorescent probes and confocal microscopy. J. Biol. Chem. *276*, 32925–32932.

Stulnig, T. M. (2003). Immunomodulation by polyunsaturated fatty acids: mechanisms and effects. Int. Arch. Allergy Immunol. *132*, 310–321.

Stulnig, T. M., Huber, J., Leitinger, N., Imre, E. M., Angelisova, P., Nowotny, P., and Waldhausl, W. (2001). Polyunsaturated eicosapentaenoic acid displaces proteins from membrane rafts by altering raft lipid composition. J. Biol. Chem. *276*, 37335–37340.

Vacca, F., Amadio, S., Sancesario, G., Bernardi, G., and Volonte, C. (2004). P2X3 receptor localizes into lipid rafts in neuronal cells. J. Neurosci. Res. *76*, 653–661.

Yan, H., and Tsai, M. -D. (1999). Nucleoside monophosphate kinases: structure, mechanism, and substrate specificity. Adv. Enzymol. Relat. Areas Mol. Biol. *73*, 103–134.

Yegutkin, G. G., Henttinen, T., and Jalkanen, S. (2001). Extracellular ATP formation on vascular endothelial cells is mediated by ecto-nucleotide kinase activities via phosphotransfer reactions. FASEB J. *15*, 251–260.

Yegutkin, G. G., Henttinen, T., Samburski, S. S., Spychala, J., and Jalkanen, S. (2002). The evidence for two opposite, ATP-generating and ATP-consuming, extracellular pathways on endothelial and lymphoid cells. Biochem. J. *367*, 121–128.

Zimmermann, H. (2000). Extracellular metabolism of ATP and other nucleotides. Naunyn Schmiedebergs Arch Pharmacol. *362*, 299–309.